1967

A Comparison of (P,2n) and (P,Pn) Reactions on Cerium-140 at Intermediate Energies

Thomas Jean Ruth
College of William & Mary - Arts & Sciences

A Comparison of (p,2n) and (p,pn) Reactions on Cerium-140 at Intermediate Energies

---

A Thesis

Presented to

The Faculty of the Department of Chemistry

The College of William and Mary in Virginia

In Partial Fulfillment

Of the Requirements for the Degree of

Master of Arts

---

by

Thomas J. Ruth

1967

APPROVAL SHEET

This thesis is submitted in partial fulfillment of

the requirements for the degree of

Master of Arts

Author

Approved, August 1967

Richard L. Kiefer, Ph.D.

Joseph T. Zung, Ph.D.

S. Young Tyree, Ph.D.

ACKNOWLEDGEMENTS

The author wishes to express his appreciation to Professor Richard L. Kiefer for his guidance and helpful discussions. Thanks is also due to the cyclotron crew at the Space Radiation Effects Laboratory (SREL) for carrying out the irradiations and to Mr. Edward Katz whose assistance and discussions were greatly appreciated.

The author is indebted to the College of William and Mary for a research assistantship and to the National Aeronautics and Space Administration for financial support which made this research possible.

TABLE OF CONTENTS

ABSTRACT

A comparison is made between the (p,2n) and (p,pn) reactions on Ce^{140} at energies between 300 and 550 MeV. The cross sections for the (p,pn) reaction were constant at approximately 86mb which compared favorably with those reported in the literature. The (p,2n) cross sections not previously reported show a decline from 52.4 mb at 300 MeV to 7.8 mb at 400 MeV and remain relatively constant from there to 500 MeV.

LIST OF TABLES AND FIGURES

A Comparison of (p,2n) and (p,pn) Reactions on Cerium-140 at Intermediate Energies

INTRODUCTION

A nuclear reaction is a process in which a projectile interacts with an atomic nucleus producing one or more other nuclei and possibly other particles. The projectile is usually another nucleus or a neutron. Reactions induced by projectiles with kinetic energy below 100 MeV can best be described as an amalgamation of projectile and target, a process called compound nucleus formation. Above 100 MeV the nuclear reactions seem to proceed by different processes. This is made evident by the fact that the mean free path of a proton of these energies is on the order of 10^{-13}cm which is of the same order of magnitude as nuclear radii. Therefore it is possible for a high energy proton to make only a few collisions while traversing a complex nucleus, leaving behind only a fraction of its energy and sometimes directly ejecting a nucleon with which it collides (4). The struck nucleons often have considerable kinetic energy and their passage through the nucleus can be considered in the same manner as the incident particle, thus forming a so called intranuclear cascade of knock-on reactions. The overall reaction, then can be thought of as occurring in two stages (4):

1) The knock-on cascade in which one or more particles are directly ejected from the nucleus leaving behind the cascade product in an excited state.

2) Subsequent deexcitation of the cascade products which may occur in at least two ways:

a. The residual excited nucleus losing nucleons or clusters of nucleons in a process similar to that of the evaporation of molecules from a water drop.

b. The excited cascade product may divide into two roughly equal pieces in a manner that is analogous to a fission process.

In order to better understand the make-up of the nucleus and the reasons for these complex reactions occurring, it is desirable to study simple nuclear reactions. These are reactions induced by a nucleon (proton or neutron) with one or two nucleons ejected, for example (p,n), (p,pn), (n,2n), etc.

Grover and Caretto (6) list the following mechanisms by which a simple nuclear reaction above 100 MeV may follow:

(1) Clean knock-out, in which the incident particle penetrates the nucleus, interacts with one of the nucleons and the two collision partners emerge without further disturbance of the nucleus.

(2) Unclean knock-out, in which the incident particle penetrates the nucleus with interaction among the nucleons which is followed by the expulsion of two nucleons in a fast process.

(3) Inelastic scattering (ISE), followed by evaporation of a nucleon, in which a nucleon of the same

type as the incident particle but with less energy emerges promptly followed by another nucleon at a much later time.

(4) Charge-exchange scattering, followed by evaporation (CESE) of a nucleon. A nucleon of the opposite type from the incident particle emerges promptly followed by a nucleon at a much later time.

(5) Compound nucleus formation, followed by slow evaporation of two nucleons.

A reaction involving an incident proton with the ejection of two neutrons (p,2n) is of interest because the incident particle does not come out. Also this type of reaction has not been studied much. A comparison of this reaction (p,2n) with a reaction involving an incident proton with the ejection of a proton and a neutron (p,pn) could lead to information on the mechanisms which they follow.

Cerium-140 was chosen as a target material for many reasons. The (p,pn) and (p,2n) reactions can be studied in the same experiment. The Ce^{140} (p,pn) Ce^{139} reaction has been previously studied (1). The Ce^{140} (p,2n) Pr^{139} reaction has not been reported with incident particles with kinetic energy above 100 MeV. The 4.9 hour half-life of Pr^{139} (11) was convenient as far as allowing time to perform the chemistry and compile data. The half-life of Ce^{139} is 140 days. Target material enriched in Ce^{140} was obtainable and a technique for the separation of cerium from praseodymium had been established.

The decay schemes for Pr^{139} and Ce^{139} are shown in Figs. 1 and 2 respectively.

The reaction cross sections were based on the accepted values for the cross section of the monitor reaction Al^{27} (p,3pn) Na^{24} (2).

Figure 1

Decay Scheme of Praseodymium-139

from Reference 11

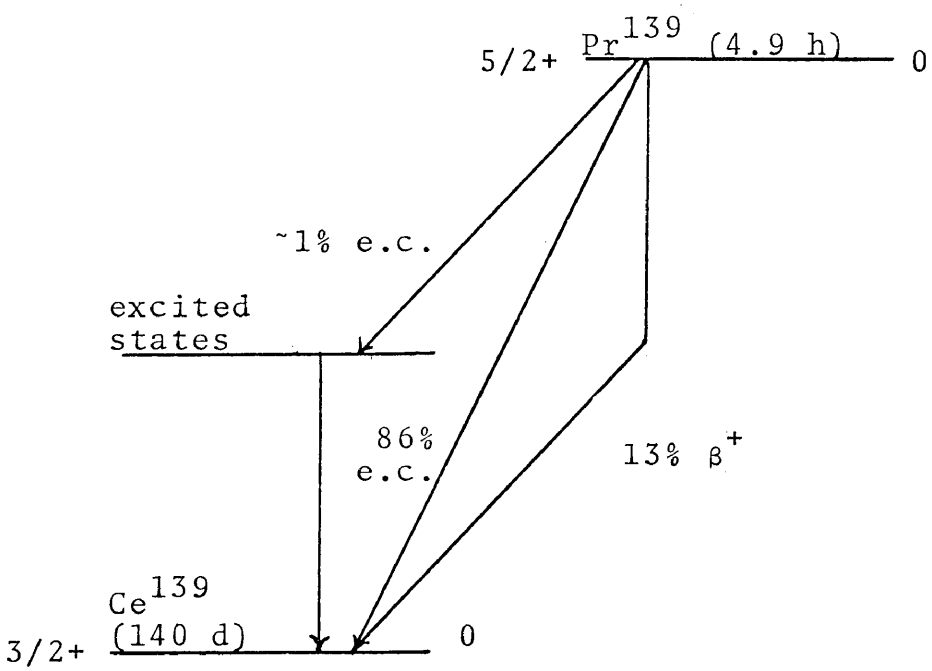

Figure 2

Decay Scheme of Cerium-139

from Reference 4

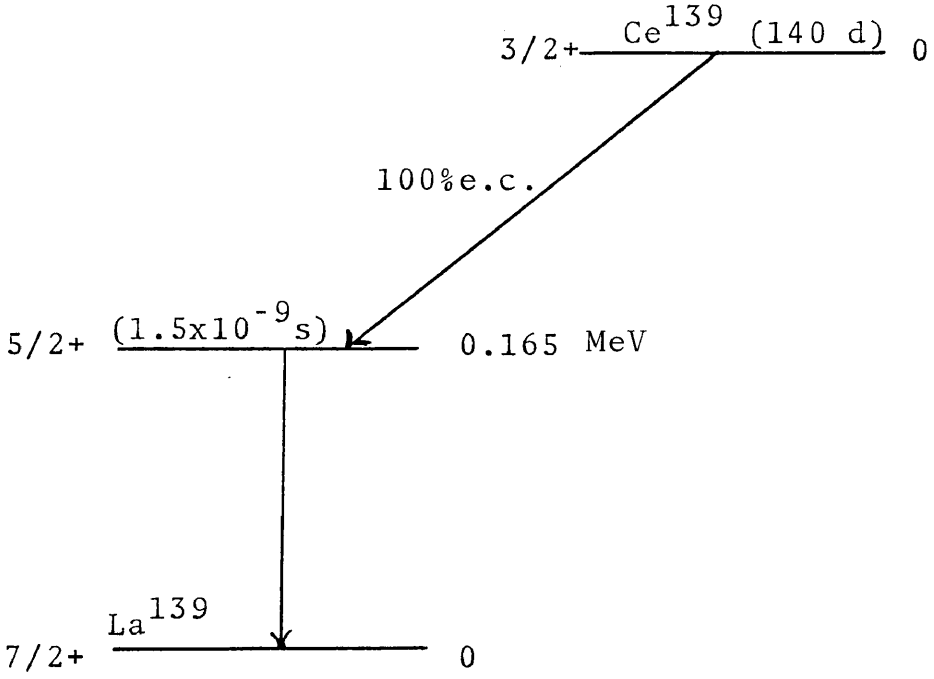

II. PROCEDURE

A. Target Preparation

The targets were prepared by depositing a film of CeO_2 on aluminum foil of known thickness (1.5 mil) and area (2"x2"). The CeO_2, obtained from Oak Ridge National Laboratory, contained 99.70% Ce^{140}. The aluminum foils were 99.99% pure. Aluminum is 100% Al^{27}.

The cerium oxide was deposited by sedimentation using a Millipore Filter apparatus with chimney. The tared aluminum foil was placed in the filter holder in the same manner as filter discs would be. The exposed area on the aluminum was measured to be 9.61 cm^2.

Approximately 10 mg. of CeO_2 was slurried with acetone and immediately poured into the chimney of the filter holder. The CeO_2 was allowed to settle and the acetone allowed to evaporate leaving a thin uniform film of CeO_2. The foil was then weighed to determine the weight of target material per square centimeter.

The foil was cut in half forming two foils with semi-circular deposits of cerium as shown in Fig. 3. The foils were sprayed with Plastiklear, a clear plastic coating

Figure 3

Detail of CeO_2 Target

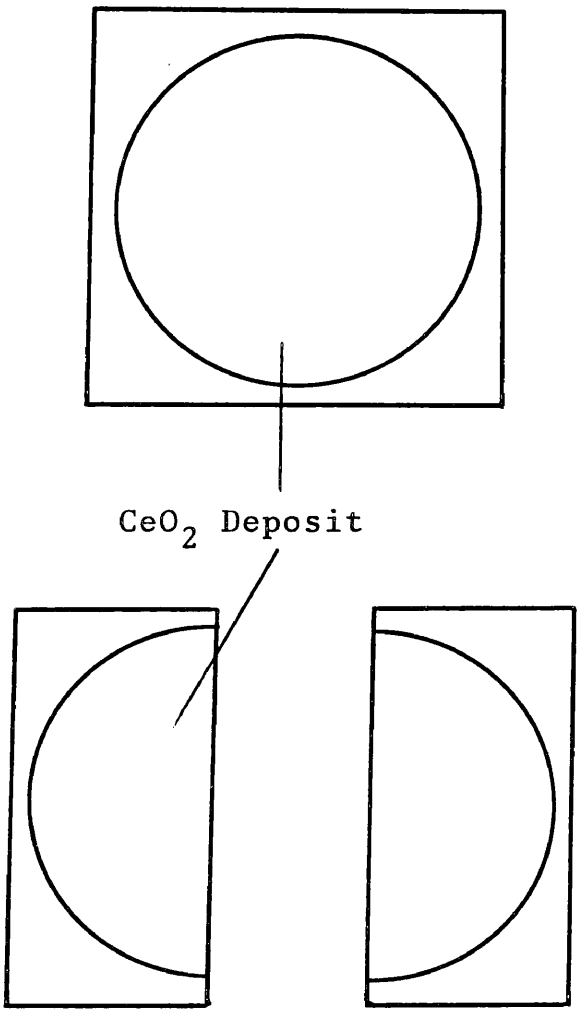

Target foil cut in half to provide two targets with even front edges.

to prevent the film from flaking off. For irradiation, a packet was made by placing the foil with the cerium between two foils of 1.5 mil aluminum. These foils monitored the beam. A 1/6 mil aluminum foil was placed between the front monitor foil and the target foil to prevent the recoil nuclei from contaminating the monitor foil. A guard foil of 1.5 mil aluminum was wrapped around the stack of foils to hold them together during irradiation (Fig. 4).

B. Irradiation

The 600 MeV synchrocyclotron at the Space Radiation Effects Laboratory (SREL) in Newport News, Virginia was used for the proton irradiations. The target packet was placed in a holder depicted in Fig. 5. The holder with target was attached to the end of the internal probe arm. The distance from the front edge of the target to the probe head was recorded.

A graph of energy versus radial distance was used to determine the distance from the center of the cyclotron to the front or leading edge of the target so that it could intercept protons of the desired energy (10).

A selection of proton energies was made between 300 MeV and 550 MeV. The ability to use protons of higher energy than 550 MeV internally was questionable because the extraction system for 600 MeV protons would intercept or at least scatter the protons before they reached the target.

Figure 4

Schematic Diagram of Target Packet

A. Target foil with cerium oxide deposit

B. 1/6 mil Al spacer foil

C. Front and rear monitors

D. Guard foil

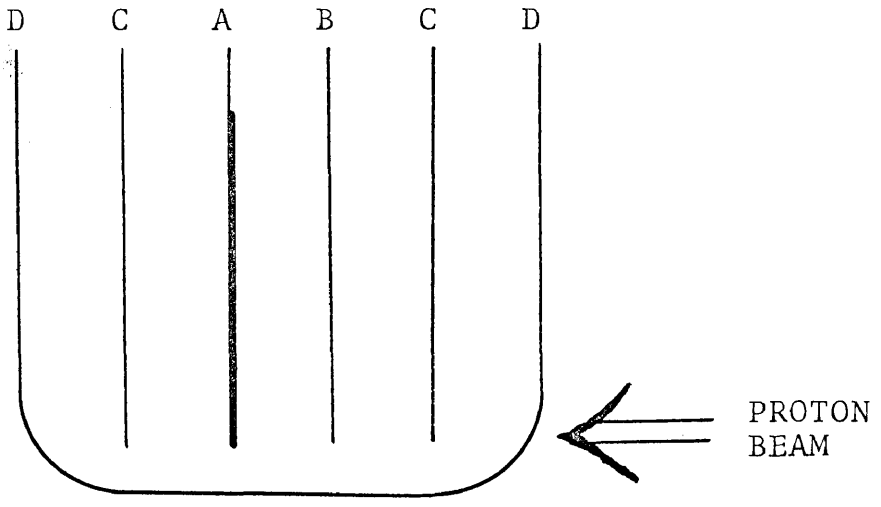

Figure 5

Target Holder Assembly

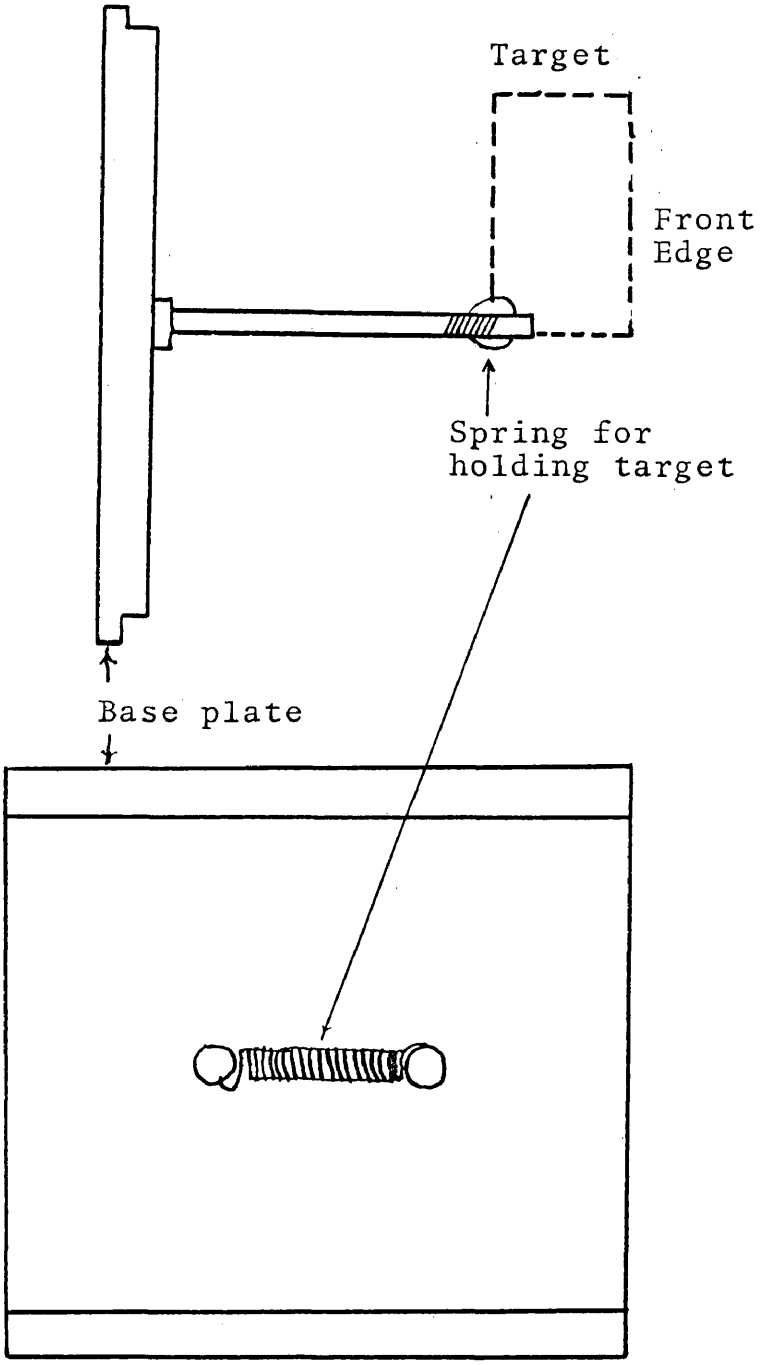

Using the activity of the monitor foils and the accepted cross section values for the Al^{27} (p,3pn) Na^{24} reaction the total number of protons incident on the target could be determined for each run. A front and rear monitor were used to detect any attenuation of the beam while traversing the target.

C. Chemistry

Since praseodymium has several isotopes with half-lives shorter than that of Pr^{139}, all of which decay to cerium, an interim period of four to five hours was used before the separations were begun. This minimized the amount of cerium in the separated praseodymium.

Figure 6 shows the activity as a function of distance from the leading edge. It is evident that the alignment of the target and monitors is essential for them to be exposed to the same number of protons. This radial dependence of activity in the target is caused by attenuation of the beam as it makes multiple traversals through the target packet. Therefore a 0.50" x 0.50" square was cut out of the target packet 1/8" from the leading edge, minimizing any error due to poor alignment of target and monitors. A modified version of the punch shown in Fig. 7 was used for the cutting. The guard foils were discarded and the monitors were placed in labeled containers for analysis later. The target foil and the spacer foil were dissolved in hot concentrated HCl. A pinch of KI was added to aid in the

Figure 6

Induced Activity in Target

vs

Distance from Front Edge

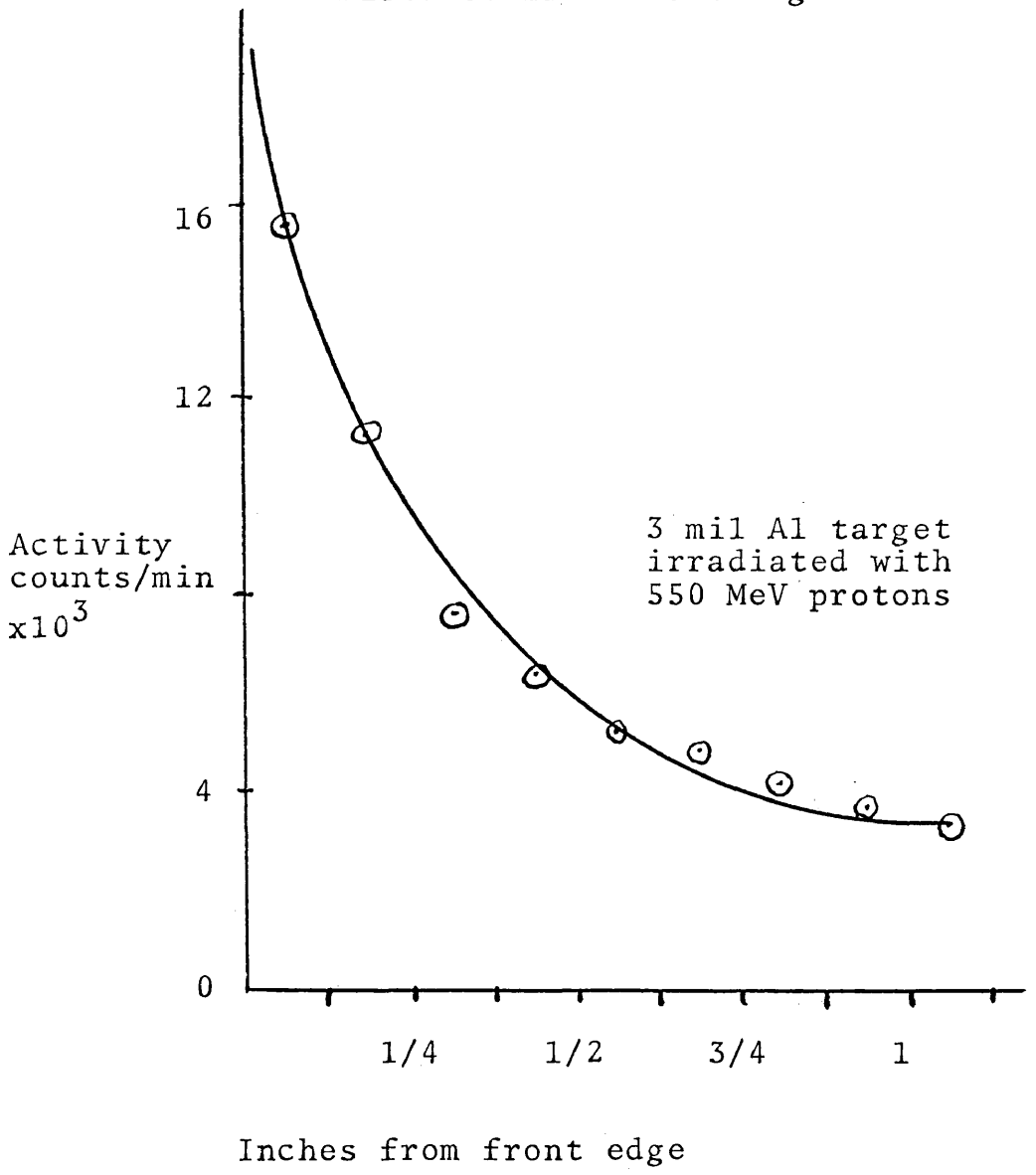

Figure 7

Punch for Cutting Irradiated Samples

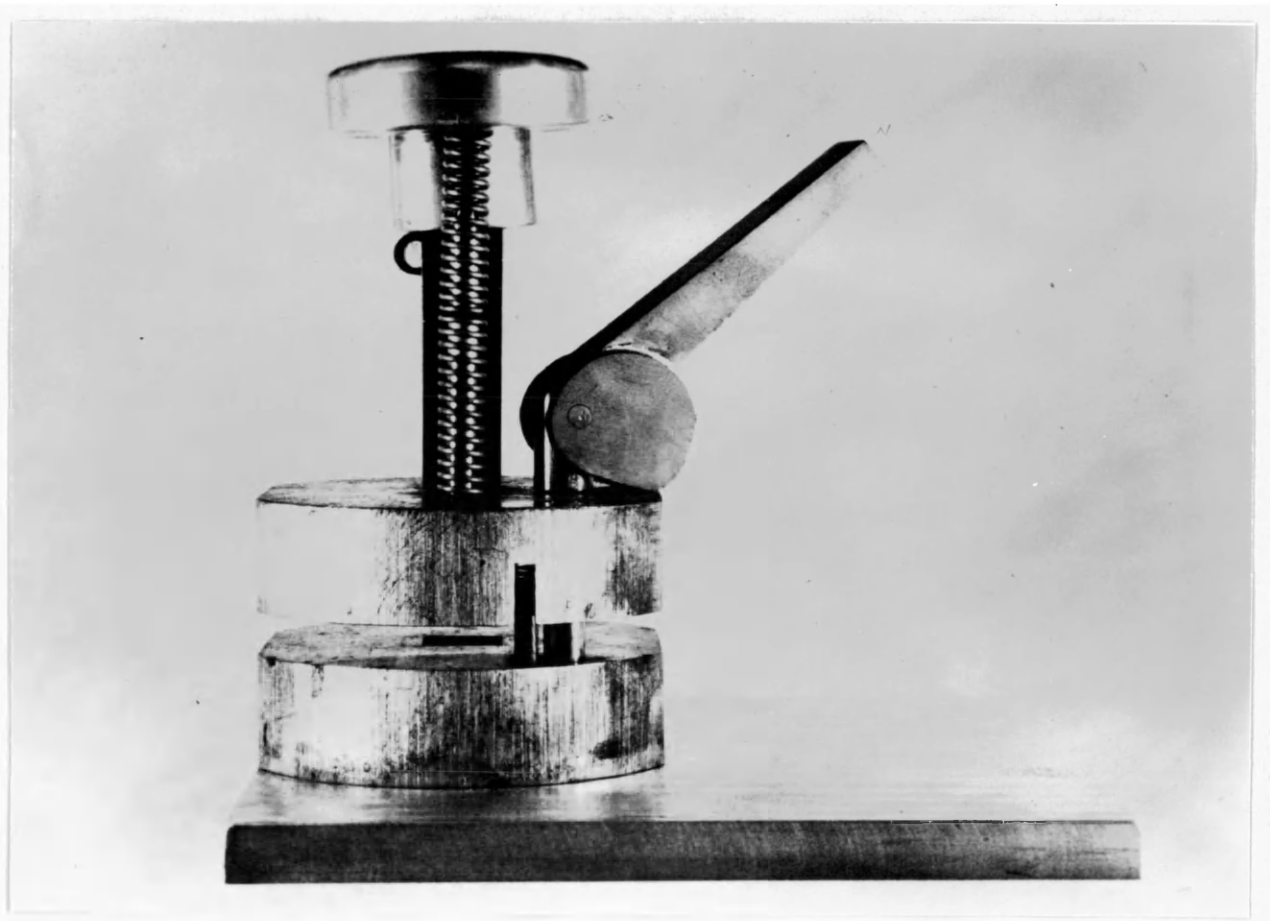

The irradiated sample is placed between the two blocks and the lever is pulled down holding the target packet secure. Then the punch is depressed, cutting a 0.50"x0.50" square 1/8" from the front edge of the packet.

reduction of CeO_2 (18).

$$2CeO_2 + 2KI + 8\ HCl \longrightarrow 2KCl + 2\ CeCl_3 + 4H_2O + I_2$$

Ten milligram aliquots of praseodymium and cerium were added as carriers. The rare earths (cerium and praseodymium) were precipitated as hydroxides by making the solution ∿10% in base which also complexed the aluminum hydroxide causing it to go into solution (12). The rare earth hydroxides were digested and filtered on fluted paper and were washed with 2% NaOH and water. The precipitate was dissolved with nitric acid and two milliliters of 5% sodium bromate was added to this solution and sufficient concentrated HNO_3 to bring the solution to 8-10M in nitric acid. This provided the environment for the oxidation of the Ce^{+3} ion to the Ce^{+4} ion. The other rare earths do not oxidize under these conditions.

The solution was poured into a separatory funnel containing methyl isobutyl ketone which had been equilibrated with nitric acid and sodium bromate to remove any reductants. The mixture was shaken for fifteen seconds and the aqueous layer was drawn off into another separatory funnel containing methyl isobutyl ketone. The aqueous phase was extracted in this manner for a total of three times. The organic phase contained the oxidized cerium (Ce^{+4}).

The aqueous phase, containing the praseodymium was neutralized with ammonium hydroxide and made slightly acid with nitric acid. The praseodymium was precipitated as the oxalate with a saturated sodium oxalate solution.

The cerium was back extracted with 30% H_2O_2 and precipated in the same manner.

The rare earth oxalates were filtered on tared #1 Whatman discs cut to fit the small Millipore filter vacuum apparatus with chimney. The precipitates were washed with acetone, allowed to dry, weighed, and mounted. The weights of the praseodymium and cerium samples were based on the fact that their oxalates contain ten and nine waters of hydration respectively (5).

The samples were always mounted in the same manner. The filter discs were centered on cardboard squares, then covered with a sheet of mylar and taped securely with plastic Scotch tape.

D. Measurement of Radioactivity

Quantitative measurements of the induced activity was determined exclusively by measurement of the characteristic x-ray of cerium or lanthanum for the Pr^{139} and Ce^{139} samples respectively. The x-ray peak was used because both samples decay primarily by electron capture as shown in Figs.1&2.

A schematic diagram of the counting apparatus is shown in Fig. 9. The detector was a Harshaw "integral line" unit which included a 3"x3" sodium iodide crystal (activated with thallium) and a photomultiplier. The voltage of the pulse (pulse height) emitted by this type of detector is proportional to the energy of the detected radiation. These pulses were amplified with a preamplifier and amplifier then analyzed

Figure 8

Spectrum Showing the X-ray from Praseodymium

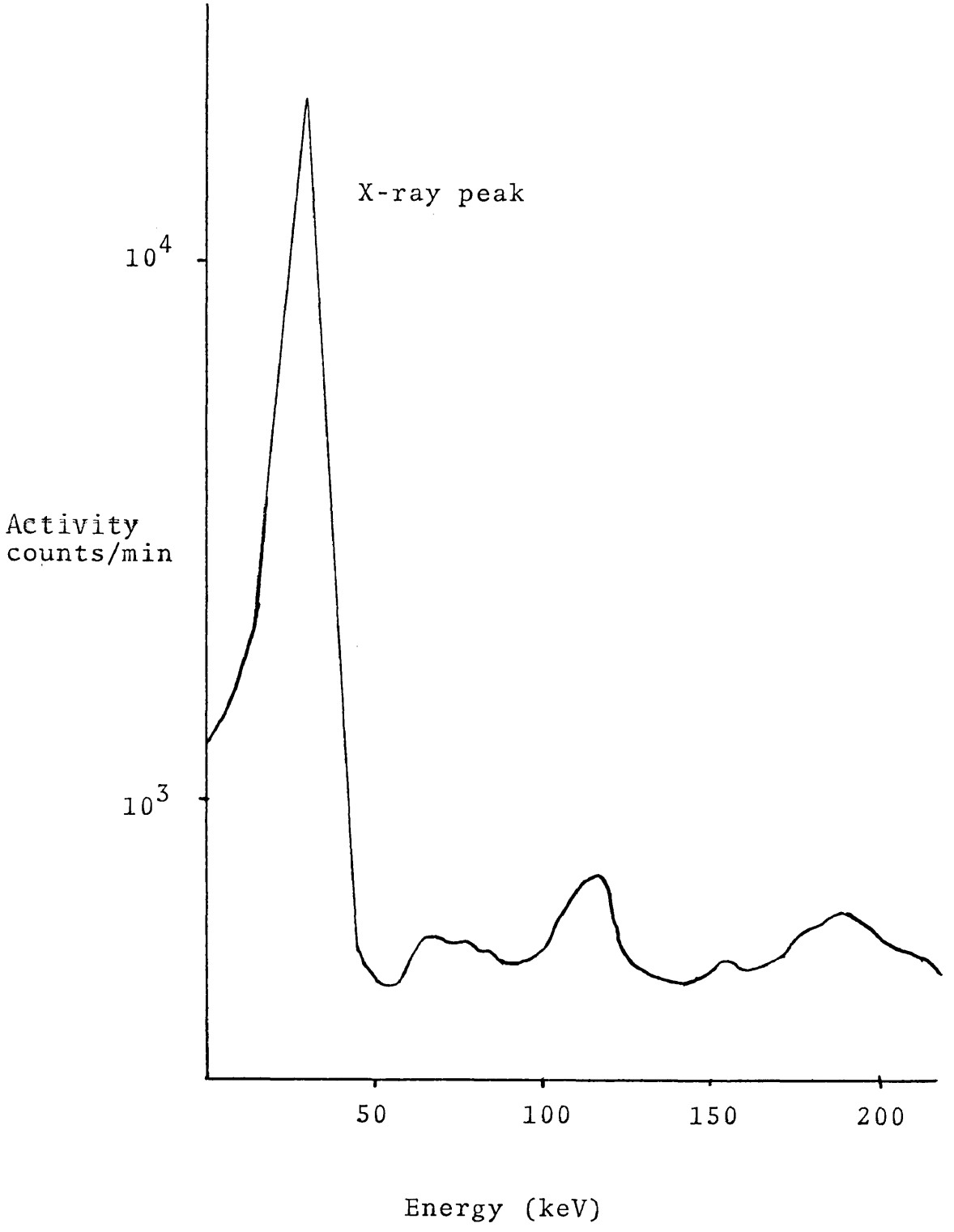

Figure 9

Schematic Diagram of Counting Apparatus

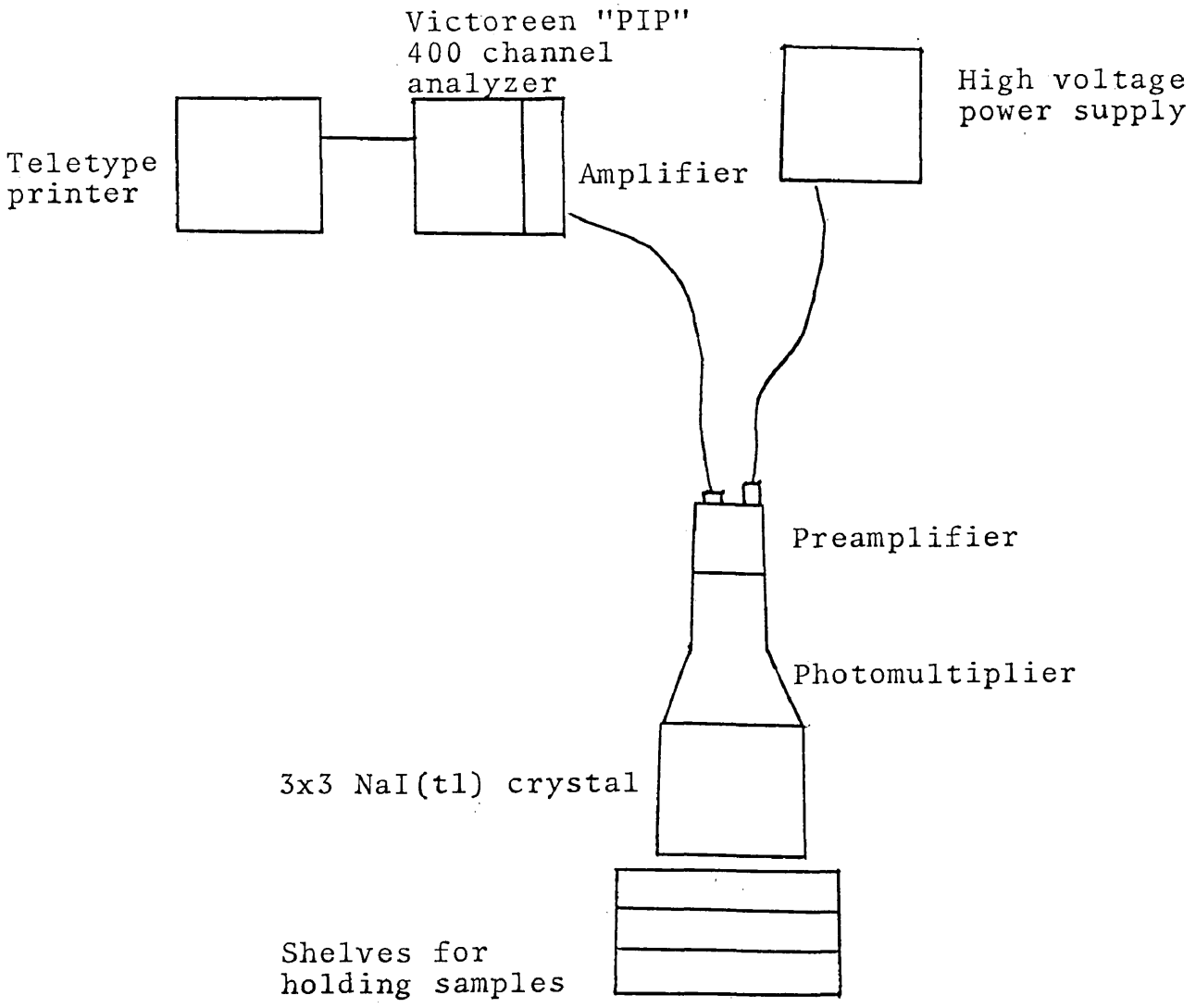

with a Victoreen "PIP", 400 channel pulse-height analyzer. The latter stored the pulses according to their pulse-height or energy. Pulses having energies within a certain energy increment were directed to the appropriate storage unit or channel. The energy increment for the channels could be preset. After the measurement, the data were recorded with a Teletype page printer. Voltage for the electrodes of the photomultiplier was supplied by a high voltage power supply.

A standardized Cs-137 source calibrated by the National Bureau of Standards was used to calibrate the counting apparatus. Tables of the efficiency of a crystal in detecting x-rays and gamma-rays for various energies were used in this calibration because Cs-137 emitts gamma-rays of 0.662 MeV and the x-rays of Pr^{139} and Ce^{139} are between 33 and 35 keV (8, 13).

E. Calculations

The number of counts in each channel was plotted against channel number or energy increment (see Fig. 8). The area under the peak was integrated and the background subtracted. These counts represented the number of photons detected during the elapsed counting time. Normalizing to counts per minute the activity was then plotted on semilog paper against the time at which the particular count was made. Radioactive decay follows the expotential law

$$N = N_o e^{-\lambda t} \quad \text{(eq. 1)}$$

where N is the number of unchanged atoms at time t, N_o is the number present at t=o, and λ is a decay constant characteristic of the particular radioactive species (4).

For a one component system such a plot would yield a straight line with the "y" intercept being equal to N_o. For a multicomponent system the plot would be a curve.

The activity due to Ce-139 was subtracted from each point before plotting. As can be seen in Fig. 10, the curve tapers into a straight line. This straight line was extrapolated back to t=o and the half-life (slope) determined by the least-squares method. Point by point this line was subtracted from the original curve to give a new curve with a straight component. This was repeated until the components were resolved. Figure 10 shows the components of the curve which were believed to be the 34 hour and 9 hour isotopes of Ce-137 and the 4.9 hour Pr-139.

With the desired component resolved it is extrapolated to time zero (time at the end of irradiation) by the least-squares method. The number of x-rays emitted at the end of irradiation is related to the number of nuclei emitting them by

$$A = c\lambda N \qquad \text{(eq. 2)}$$

where A is the activity (number of counts per minute), c is the constant related to the counting apparatus and particular nuclei under investigation, λ is the decay constant (ln2/ half-life), and N is the number of active nuclei (4).

Figure 10

Graphical Analysis of the Praseodymium Data

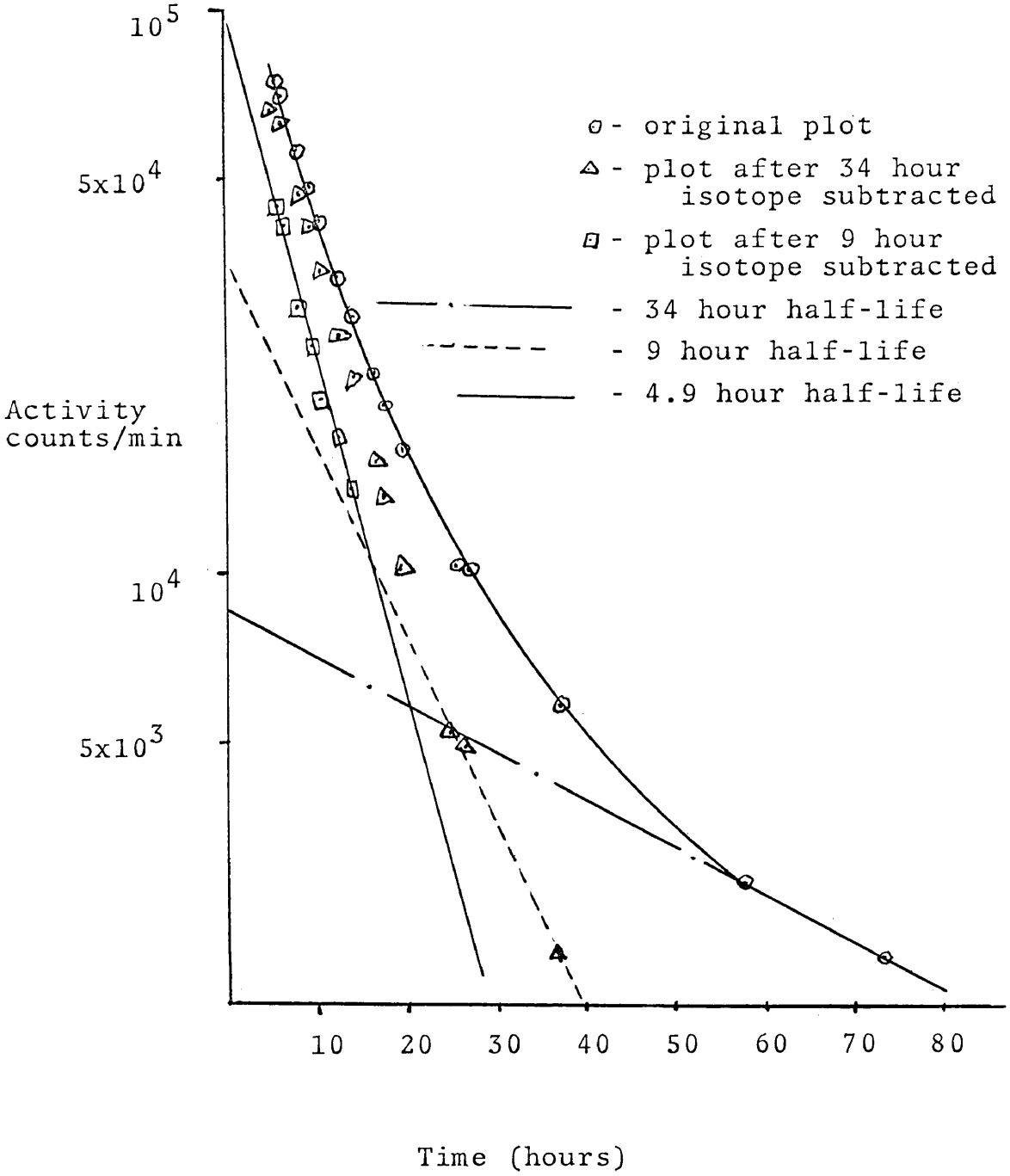

Knowing the number of nuclei found at time zero, the dimensions of the target and the number of protons incident (from the monitor observations) the cross sections were calculated from the following equation (4):

$$\sigma = \frac{N}{Inx} \quad \text{(eq. 3)}$$

where σ is the cross section for the specified process, expressed in square centimeters, N is the number of processes of the type under consideration occurring in the target, I is the number of incident particles, n is the number of target nuclei per cubic centimeter of target, and x is the target thickness in centimeters.

Because cerium-139 has a half-life of 140 days, only one count could be made. This count was made after all the shorter lived cerium isotopes had time to decay and the counts at t=o were calculated from the relationship of

$$(A=A_o e^{-\lambda t}) \quad \text{(eq. 4)}$$

where A is the activity (counts) at time t, and A_o is the activity at t=o.

At the time of chemical separation there were "N" nuclei of praseodymium (from equation 1). The number of nuclei at t=o or at the end of irradiation is N_o. The difference (N_o-N) is the amount of Pr^{139} that decayed into Ce^{139} before chemical separation was completed and amounted to ~10% of the Ce^{139} detected. This was taken into account when computing the cross sections for the reaction Ce^{140} (p,pn) Ce^{139}. For the Pr^{139} cross section, a correction

was made to account for the fact that Pr^{139} decays partially by position emission. The electron capture to β^+ emission ratio is 7.2/1 (11).

III. RESULTS

The experimentally determined values of the cross sections are given in Table 1. The errors listed are discussed below.

A plot of the cross sections versus projectile energy (excitation function) for the (p,2n) and (p,pn) reactions are shown in Fig. 11 along with the results given by Caretto (1).

The energy spread for the protons of a given energy within the cyclotron is estimated to be 3 to 4% (10).

The value of the absolute cross section of the reaction used as a monitor is uncertain by about $\pm$ 10% (2). The uncertainties in the counter efficiency and chemical yield is estimated to be $\pm$ 4% and $\pm$ 10% respectively. The graphically resolved decay curve uncertainty is estimated to be $\pm$ 15%. The error which is taken to be the square root of the sum of the squares of the pertinent uncertainties is $\pm$ 21%.

The large source of error due to curve resolution is partially caused by poorer separation of cerium and praseodymium than anticipated. This was made evident by

TABLE 1

Cross Sections for the Reactions

Ce^{140} (p,2n) Pr^{139} and Ce^{140} (p,pn) Ce^{139}

in Millibarns (10^{-27} cm^2)

E(MeV)	(p,pn) Individual Runs	(p,pn) Ave.	(p,2n) Individual Runs	(p,2n) Ave.
300	84.2 80.7	82.4± 16.5	48.0 56.9	52.4±10.5
400	86.5	86.5± 17.3	8.4 7.2	7.8±1.6
500	85.1 81.6	83.4± 16.7	12.9 9.8	11.4±2.3
550	95.0 92.5	93.8±18.8	8.1 12.2	10.2±2.0

Figure 11

Excitation Function for the

(p,2n) and (p,pn) Reaction on Ce^{140}

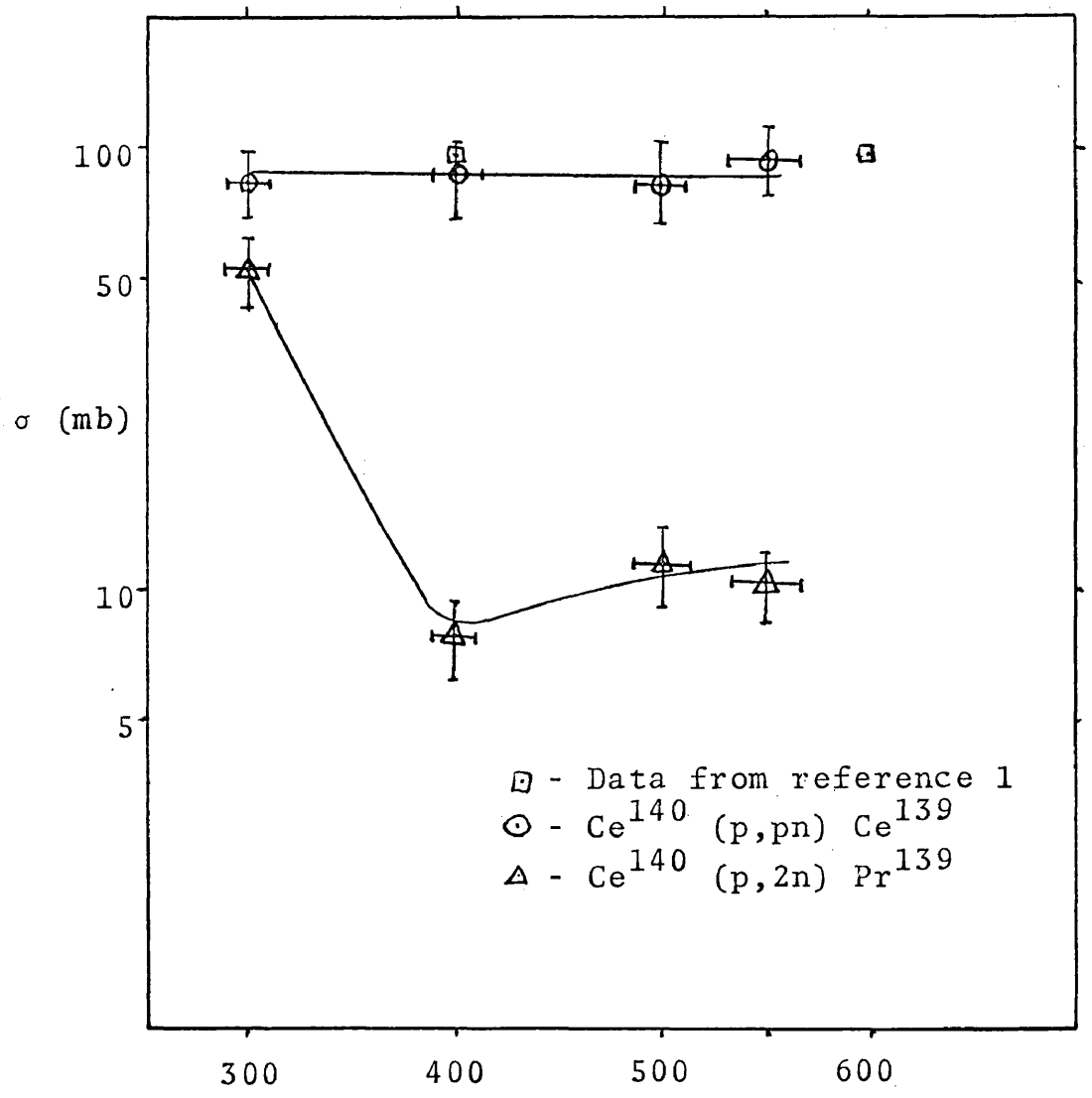

the amount of Ce^{137} produced. Cerium-137g and cerium-137m have half-lives of 34 hours and nine hours respectively. Cerium-137 is a decay product of 1.5 hour Pr^{137} which should have decayed substantially before the chemistry was performed. Foreman reports the use of potassium peroxydisulfate instead of sodium bromate (3). He indicates that bromate does not always yield complete oxidation of cerium. It is possible, however, that the Ce^{140} (p,4n) Pr^{137} reaction may have a high enough cross section to produce substantial amounts of Pr^{137} at these energies (14).

IV. DISCUSSION

From the excitation curve for the (p,2n) reactions, it can be seen that there is a marked drop in cross section between 300 and 400 MeV. This is followed by a nearly constant value up to 550 MeV. The reported excitation functions of other (p,2n) reactions show a decrease with increasing energy approximately as $(\text{energy})^{-1}$ between 100 and 400 MeV (6). Other works indicate a relatively constant cross section from 500 MeV to about 1.5 GeV (1). However, this work shows a variation in cross section between 300 and 400 MeV approximately four times that expected on the basis of $(\text{energy})^{-1}$. It is not clear why this occurs.

The (p,2n) reaction can occur through a two-step mechanism involving the direct emission of two neutrons. However, from the angular distribution and kinetic energy of the emerging neutrons, it is most probable that the CESE contributes most to this reaction (6). The effect of the evaporation step is most probably only weakly dependent on the incident energy (6). This conclusion is strongly supported by the similar energy dependence (decrease as $(\text{energy})^{-1}$) of the (p,n) reaction cross sections. Therefore,

this energy dependence appears to be a property of charge-exchange scattering. This process itself is probably the passing of a π^+ meson from the incident proton to a neutron in the nucleus. It is believed that pi-mesons are the particles that are exchanged between two nucleons resulting in nuclear forces. It can be considered analogous to chemical forces which depend on the exchange of an electron between two atoms. However, mesons are "virtual" particles which are created at the instant of emission from one nucleon and vanishes at the instant of absorption by the other nucleon (4). The threshold energy for the creation of pi-mesons is approximately 280 MeV. Once the threshold energy for creation of the actual particle has been reached, the pion could escape from the nucleus along with the incident particle. At the threshold energy, the pion does not have sufficient energy to leave the nucleus. However, above about 300 MeV it can be expected that simple nuclear reactions can include such reactions as $(p,p\pi^-)$, (p,π^0n), $(p,pn\pi^-)$, <u>etc</u> (6). Thus, a $(p,pn\pi^-)$ reaction would lead to the same product as a (p,2n) reaction while $(p,2n\pi^+)$ and $(p,2p\pi^-)$ reactions would appear as a (p,pn) reaction. However, in the creation of a pion at least 280 MeV is expended. Therefore, pion formation would not be expected to contribute much to these reactions below 400 MeV. Although the cross section for the formation of pions increases rapidly with energy above 400 MeV, the percentage contribution is unknown.

The (p,pn) reaction can follow the clean knock-out, ISE, or the unclean knock-out mechanisms, with the clean knock-out being the most probable (6). From experimental data and calculations, Grove and Caretto suggest that the clean knock-out and ISE mechanisms contribute ~65% and ~30% respectively to the total cross section for a (p,pn) reaction.

In studies of cross sections for the interaction of a proton with a free neutron, it was found that the p-n cross section remains constant within $\pm$ 10% in the energy region of 300 to 600 MeV (14). The (p,pn) reaction cross sections reported in the literature (1, 6) are also roughly constant for this energy region, as are the data from this work. From experimental evidence one can assume that the clean knock-out process is analogous to the interaction of free nucleons (14). Ware and Wiig calculate an energy dependence for the ISE mechanism of about $(\text{energy})^{-0.6}$ for the Ce^{140} (p,pn) Ce^{139} reaction in this energy region (19). Thus, it appears that the clean knock-out process is the predominant mechanism for the (p,pn) reaction at these energies.

Winsberg speculates from experimental data that one should expect about an order of magnitude difference between so called one-step and two-step mechanisms (13). Assuming this is to be true, the experimental data indicate that the (p,pn) reaction proceeds by a one-step mechanism and the (p,2n) reaction proceeds by a two-step mechanism. At 300 MeV, however, cross sections for the two reactions are much closer together. It is not clear why this occurs.

In the monitor studies there was little if any attenuation between the forward and rear monitors making it possible to assume that the cerium target was being subjected to the same number of protons as the monitors were.

During half of the irradiations, the magnet was used with reverse field causing the protons to travel in the opposite direction. The target was always placed in the holder in such a manner that the cerium oxide deposit would face the in-coming protons. There was no apparent effect on the beam strength or on the cross sections from the field reversal.

V. CONCLUSION

In light of the reasonable comparison of the experimental and reported values for the (p,pn) reaction, it can be assumed that the beam has been monitored with sufficient effectiveness to give representative data for the (p,2n) reaction.

It appears that the two reactions follow different mechanisms. The (p,pn) reaction is relatively energy independent while the (p,2n) reaction is very energy dependent at lower energies. There is also a difference in the cross section values for the two reactions. Although the (p,2n) reaction follows the general trend of the other (p,2n) reactions, it is markedly different at lower energies. This cannot be explained at this time.

From the compiled data of Grover and Caretto, the dependence of the cross sections of the (p,2n) reactions on mass appears to be erratic (6). Perhaps there is a strong mass dependence in this region. Only further investigation with nuclides in this mass region of the (p,2n) reaction in conjunction with the (p,xn) reaction can shed light on the complex problem of the energy dependence. It would also be helpful to investigate the Ce^{140} (p,2n) Pr^{139} reaction at lower energies, between 100 and 300 MeV.

BIBLIOGRAPHY

1. Caretto, A.A., Jr., AEC Rept. NYO-10693 (1964).

2. Cumming, J.B., Ann. Rev. Nucl. Sci. 13, 261 (1963).

3. Foreman,B.M., Jr., Phys. Rev., 132,1768 (1963).

4. Friedlander, Gerhart, Joseph W. Kennedy, and Julian Malcom Miller, Nuclear and Radiochemistry, New York, London, John Wiley and Sons, Inc. (1964).

5. Glendenin, L.E., K.F. Flynn, R.F. Buchanan, and E.P. Steinberg, Anal. Chem. 27, 59 (1955).

6. Grover, J. Robb and A.A. Caretto, Jr., Ann. Rev. Nucl. Sci. 14, 51 (1964).

7. Handly, T.H. and E.L. Olson, Phys. Rev. 96, 1003 (1954).

8. Heath, R.L., Scintillation Spectrometry Gamma Ray Spectrum Catalogue, AEC Research and Development Report 100-16880, (1964),

9. Hillman, Manny, An Extended Table of Nuclidic Masses, BNL846 (T-333) (1964).

10. Hopp, David, (Virginia Associated Research Center) private communication.

11. King, J.D., (Physics Department, University of Toronto, Toronto, Canada) private communication.

12. Kothoff, I.M. and Philip J. Elving, Treatise on Analytical Chemistry, New York, London: Interscience Publishers, (1961) Vol. 8, p. 36.

13. Ladenbauer, I., and L. Winsberg, Phys. Rev. 119, 1368 (1960).

14. Meloni, S., and J.B. Cumming, Phys. Rev. 136, B1359 (1964).

15. Mott, W.W. and R.B. Sutton, S. Fligge and E. Creuty, eds. Handbuch der Physik. Berlin: Springer (1958) Vol. XLV, p. 113.

16. Porile, Norbert T., Phys. Rev. 125, 1379 (1962).

17. Stover, B.J., Phys. Rev. 81, 8 (1951).

18. Treadwell, F.P., Analytical Chemistry. New York: John Wiley and Sons, Inc. (1935) Vol. II, p. 612.

19. Ware, W.R. and E.O. Wiig, Phys. Rev. 122, 1837 (1961).

VITA

Thomas Jean Ruth

Born in Phoebus, Virginia, July 20, 1943. Graduated from Hampton High School, Hampton, Virginia, June 1960, B.S., St. Francis College, June 1964. Employed by Newport News Shipbuilding and Dry Dock Company, June 1964, as water chemist for coolant systems of nuclear naval vessels. Entered the College of William and Mary, September 1965, concentrating in Chemistry. With the course requirements completed, became M.A. Candidate, January 1967.